Eliot Chang is from Seattle, WA, and is currently a junior at Pomona College majoring in Chemistry and Environmental Analysis. Eliot's research was conducted Lawrence Berkeley National Laboratory (LBNL) in the SULI program. Eliot presented a poster on this research in the Department of Energy's Science and Energy Research Challenge (SERCh) competition in Oak Ridge, Tennessee in November 2008. He will finish his B.A. in 2010, after which he plans to spend time traveling and exploring the world before attending graduate school. In his spare time, Eliot enjoys playing and watching all kinds of sports.

Yongzhu Fu was a postdoctoral fellow at Lawrence Berkeley National Laboratory. He received his Ph.D. from the University of Texas–Austin in 2007 working on new polymer membrane materials for fuel cells. He developed a number of new membranes that show high proton conductivity and low methanol crossover in direct methanol fuel cells. He came to LBNL as a postdoc to develop new polymer membrane materials for high temperature proton exchange membrane fuel cells. His research activities have focused on imidazole-based ionic liquids, in particular the study of effect of composition on proton conductivity and property of the ionic liquids. He also developed new polymers consisting of aryl backbones and alkyl side chains with imidazole or sulfonic acid end groups.

John Kerr is presently a Staff Scientist in the Environmental Energy Technology Division of Lawrence Berkeley National Laboratory, where he is PI on a major Department of Energy effort to develop the next generation of fuel cell membranes that involves the University of California–Berkeley, researchers at Los Alamos National Laboratory and 3M. This program developed out of previous membrane work for lithium batteries, electrochromic windows and polymer LEDs for high efficiency lighting. Prior to coming to the Lab, Dr. Kerr worked with Aquanautics Corporation in Alameda on electrochemical gas separation, including the "Artificial Gill" for underwater power as well as oxygen separation and control for food packaging applications. He has also held senior research positions with PPG Industries, EverReady Batteries and Occidental Chemical. Dr. Kerr's current research areas include fuel cell membranes, high temperature membranes and catalysts, lithium polymer and lithium ion batteries, electrochemical and polymer technology for bioprocessing and biosensors, organic electrochemistry, conducting polymers and organics for OLED devices in lighting and organic PV.

Imidazole-Based Ionic Liquids for Use in Polymer Electrolyte Membrane Fuel Cells: Effect of Electron-Withdrawing and Electron-Donating Substituents

Eliot Chang, Yongzhu Fu and John Kerr

ABSTRACT

Current polymer electrolyte membrane fuel cells (PEMFCs) require humidification for acceptable proton conductivity. Development of a novel polymer that is conductive without a water-based proton carrier is desirable for use in automobiles. Imidazole (Im) is a possible replacement for water as a proton solvent; Im can be tethered to the polymer structure by means of covalent bonds, thereby providing a solid state proton conducting membrane where the solvating groups do not leach out of the fuel cell. These covalent bonds can alter the electron availability of the Im molecule. This study investigates the effects of electron-withdrawing and electron-donating substituents on the conductivity of Im complexed with methanesulfonic acid (MSA) in the form of ionic liquids. Due to the changes in the electronegativity of nitrogen, it is expected that 2-phenylimidazole (2-PhIm, electron-withdrawing) will exhibit increased conductivity compared to Im, while 2-methylimidazole (2-MeIm, electron-donating) will exhibit decreased conductivity. Three sets of ionic liquids were prepared at defined molar ratios: Im-MSA, 2-PhIm-MSA, and 2-MeIm-MSA. Differential scanning calorimetry (DSC), thermogravimetric analysis (TGA), and ^{1}H-NMR were used to characterize each complex. Impedance analysis was used to determine the conductivity of each complex. Both the 2-PhIm-MSA and 2-MeIm-MSA ionic liquids were found to be less conductive than the Im-MSA complex at base-rich compositions, but more conductive at acid-rich compositions. ^{1}H-NMR data shows a downfield shift of the proton on nitrogen in 2-PhIm compared to Im, suggesting that other factors may diminish the electronic effects of the electron withdrawing group at base-rich compositions. Further studies examining these effects may well result in increased conductivity for Im-based complexes. Understanding the conductive properties of Im-derivatives due to electronic effects will help facilitate the development of a new electrolyte appropriate for automotive fuel cell use.

Introduction

As the effects of global climate change are becoming more clear, a changing energy landscape has resulted in an increased demand for alternative energy. An emerging clean-energy technology is the fuel cell, which possesses the potential to replace internal combustion engines in automobile systems. However, fuel cell technology must still be adapted for high performance in automobiles [1]–[3]. Polymer electrolyte membrane fuel cells (PEMFCs) are particularly strong candidates due to their high energy-conversion efficiency, low operating temperatures, and zero emission potential [4]. However, membrane technology must be modified for fuel cells to run efficiently within vehicles before they are competitive for automotive commercialization.

The distinguishing feature of PEMFCs is the polymer electrolyte, which separates the cathode, anode, and reactants while maintaining high proton conductivity (Figure 1). The most common commercially available fuel cells on the market today employ Nafion®, produced by DuPont®, a perfluoronated sulfonic acid polymer with good thermal and chemical stability as well as high proton conductivity. Since water molecules act as the vehicle for proton transport in the membrane, Nafion® requires constant humidification and an operating temperature below the vaporization point of water (100 °C). Due to inefficiencies in the catalyst performance, a significant amount of heat is generated by the fuel cell. Any excess heat beyond 100 °C must be removed by a cooling system. Current automotive cooling systems are designed to operate around 120 °C, creating an environment that is incompatible with current fuel cells. Recent research has focused on the development of a polymer which conducts protons at a high temperature (>100° C) and low humidity [5]–[8]. The benchmark goal for a practical polymer is set at 0.1 S/cm at 120 °C by the U.S. Department of Energy (DOE).

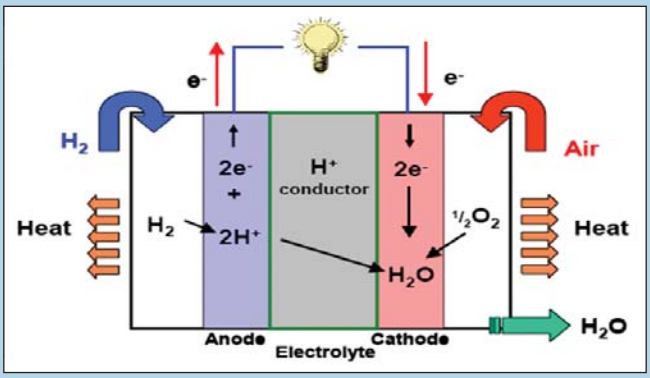

Figure 1. Schematic of a polymer electrolyte membrane fuel cell.

One molecule which has attracted considerable attention as an alternative to water for proton transport is imidazole (Im). Im and its derivatives have been shown to be good Brønsted acids and bases, transporting protons by means of vehicular solvent motion and by the Grotthuss mechanism [9], wherein the protons are transferred by hopping from site to site in a long chain of Im-containing complexes (Figure 2). Unlike Nafion®, Im-based membranes are conductive under anhydrous conditions, demonstrating a potential for the adaptation of fuel cell technology for automotive uses. However, measured conductivities are lower than desired, and the development of a replacement polymer continues. Recent research has investigated several Im-based compounds with various functional groups which could be used at 120 °C and low humidity, but a replacement for Nafion® has not yet been produced [10]–[11].

Considering the laborious process of polymer synthesis, ionic liquids can serve as preliminary compounds upon which polymers may be modeled. Proton-conducting ionic liquids are salts composed of an acid/base pair; they have high proton conductivity but lack the ordered structure provided by a polymer backbone. The acid provides a source of protons while the base, typically a heterocyclic compound, provides a means of proton transfer through solvation. Not only must the acid/base pair be carefully selected but

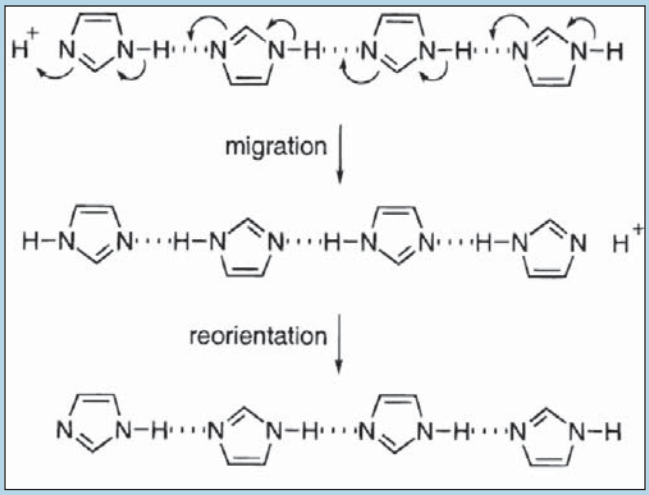

Figure 2. Grotthuss mechanism of proton transport for Im. Source: [14]

proper molar ratios must also be maintained to maximize proton conductivity.

This study examines the effect of electron-withdrawing and electron-donating groups on the conductivity of Im-based ionic liquids. Im, 2-methylimidazole (2-MeIm), and 2-phenylimidazole (2-PhIm) are complexed with methanesulfonic acid (MSA) at defined molar ratios (Figure 3). Altering the electron density of the lone pair on nitrogen may increase the proton accepting and donating potential of Im. Impedance analysis is used to determine the conductivity of each ionic liquid at operating temperatures of 30–130 °C. The thermal properties are determined using differential scanning calorimetry (DSC) and thermogravimetric analysis (TGA). Proton nuclear magnetic resonance (^{1}H-NMR) is used to characterize the chemical shift of selected protons.

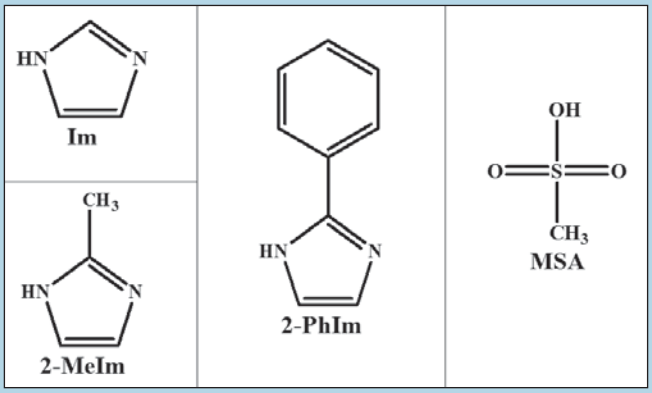

Figure 3. Molecular structure of Im, 2-MeIm, 2-PhIm, and MSA.

The electron donating (methyl) and electron-withdrawing (phenyl) groups are postulated to have different effects on proton conductivity of the complexes they form with MSA. The phenyl group is expected to reduce the electron density of the lone pair on nitrogen. The resulting weaker covalent bonds formed between Im and protons may increase the ease in which Im facilitates proton transport. However, steric hindrance due to bulky substituents could hinder the transfer of protons, thus reducing the overall conductivity. The successful development of an ionic liquid with acceptable proton

conductivity and thermal stability may help fuel cell technology realize its full potential in transforming the automotive industry.

Materials and Methods

Im (Fluka, 99.9%), 2-MeIm (Aldrich, 99%), 2-PhIm (Aldrich, 98%), and MSA (Aldrich, 99.5%) were used as received. Mixtures containing predetermined molar ratios of the Im-derivatives and MSA were heated above their respective melting temperatures to ensure homogenization for the ionic liquid complexes. All of the samples were handled and stored in a glovebox with a helium atmosphere.

Thermal Properties

Differential scanning calorimetry (DSC) was performed using a Perkin Elmer Differential Scanning Calorimeter 7 under a helium atmosphere. The samples were sealed in aluminum pans under a helium atmosphere in the glovebox before analysis. Thermograms were recorded during subsequent cooling and heating cycles. The samples were scanned at a rate of 10 °C min^{-1} within the temperature range of 100–150 °C for base-rich compositions, 50–250 °C for equimolar compositions, and 150–100 °C for acid-rich compositions. The melting temperatures (T_m, onset of endothermic peak), crystallization temperatures (T_c, onset of exothermic peak), glass-transition temperatures (T_g), and heat of fusions (ΔH) were determined by the average of two cooling and heating cycles. High temperature stability measurements were conducted using a Perkin Elmer Thermogravimetric Analyzer 7 within the temperature range of 30–500 °C at a heating rate of 5 °C min^{-1} under a nitrogen atmosphere in open platinum pans.

Ionic Conductivity

The ionic conductivity was determined using an impedance analysis method within the temperature range 130–30 °C in an oven. The samples were allowed to thermally equilibrate for at least 30 minutes prior to the impedance measurement. The measurements were taken on a cell where the ionic liquid was confined between two stainless steel electrodes separated by a polypropylene spacer. The cell was sealed inside the glovebox. The measurements were performed with a Gamry Instruments Reference 600 Potentiostat/Galvanostat/Zero Resistance Ammeter (ZRA) over a frequency range of 5 000–65 000 Hz. The conductivity was calculated from the measured resistance (x-intercept of Nyquist plot) using Ohm's Law.

^{1}H-NMR Spectra

The ^{1}H-NMR spectra were obtained by a Bruker AVQ-400 spectrometer at 400 MHz. Each sample was dissolved in dimethyl-*d6* sulfoxide (DMSO-*d6*, 99.9%-d). The measurements were conducted at room temperature.

Results

The melting temperatures (T_m), crystallization temperatures (T_c), and glass-transition temperatures (T_g) for the Im-MSA ionic liquids obtained by DSC are listed in Table 1. T_m was highest for the equimolar composition at 179.08 °C, and a T_g was only present in acid-rich compositions. The heats of fusion of the ionic liquids Im-MSA 5:5, 8:2, 4:6, 2-MeIm-MSA 8:2, 4:6, and 2-PhIm-MSA 8:2, 4:6 are listed in Table 2. The equimolar salt had the highest heat of fusion at 64.23 J g^{-1}; base-rich compositions had higher heats of fusion than acid-rich compositions. Thermal stabilities at high temperatures are shown in Figure 4 for Im-MSA ionic liquids. Im-rich compositions showed two step weight losses, the first around 150 °C, the second around 300 °C.

Mol Fraction Im	T_m [°C]	T_c [°C]	T_g [°C]
1	91.97	46.92	–
0.9	47.76	21.27	–
0.8	61.06	24.86	–
0.7	47.04	17.64	–
0.6	47.38	14.97	–
0.5	179.08	177.62	–
0.4	-6.74	–	–
0.3	–	–	-76.22
0.2	–	–	-88.6
0.1	–	–	-93.88

Table 1. Thermal properties of Im-MSA ionic liquid compositions.

Sample	ΔH [J g^{-1}]
Im-MSA 5:5	64.23
Im-MSA 8:2	19.48
2-MeIm-MSA 8:2	47.67
2-PhIm-MSA 8:2	6.35
Im-MSA 4:6	8.48
2-MeIm-MSA 4:6	1.24
2-PhIm-MSA 4:6	–

Table 2. Selected heats of fusion of Im-MSA, 2-MeIm-MSA and 2-PhIm-MSA ionic liquid compositions.

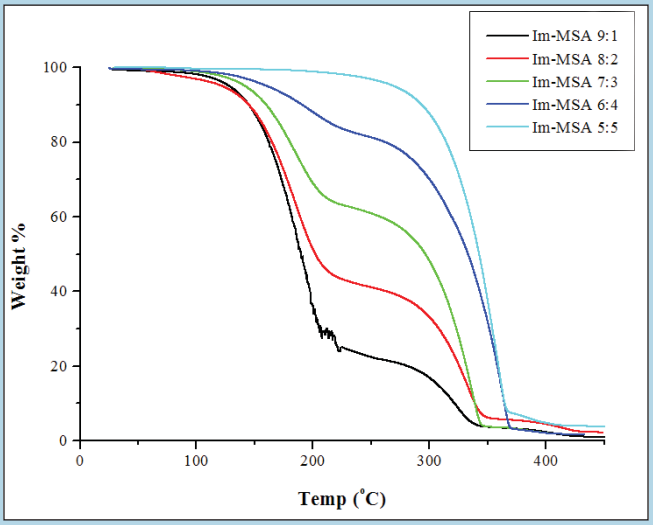

Figure 4. High temperature stabilities for Im-MSA ionic liquids.

The ^{1}H-NMR spectra for Im-MSA 8:2, 6:4, 4:6 and 2:8 ionic liquids are shown in Figure 5. Four distinct peaks are present, representing the three unique proton environments on Im and the one unique proton environment on MSA. Figure 6 compares the chemical shift of the acidic proton on MSA for Im-MSA, 2-MeIm-MSA, and 2-PhIm-MSA at a 4:6 molar ratio. The proton in the 2-PhIm-MSA complex is farthest upfield, while the proton in the

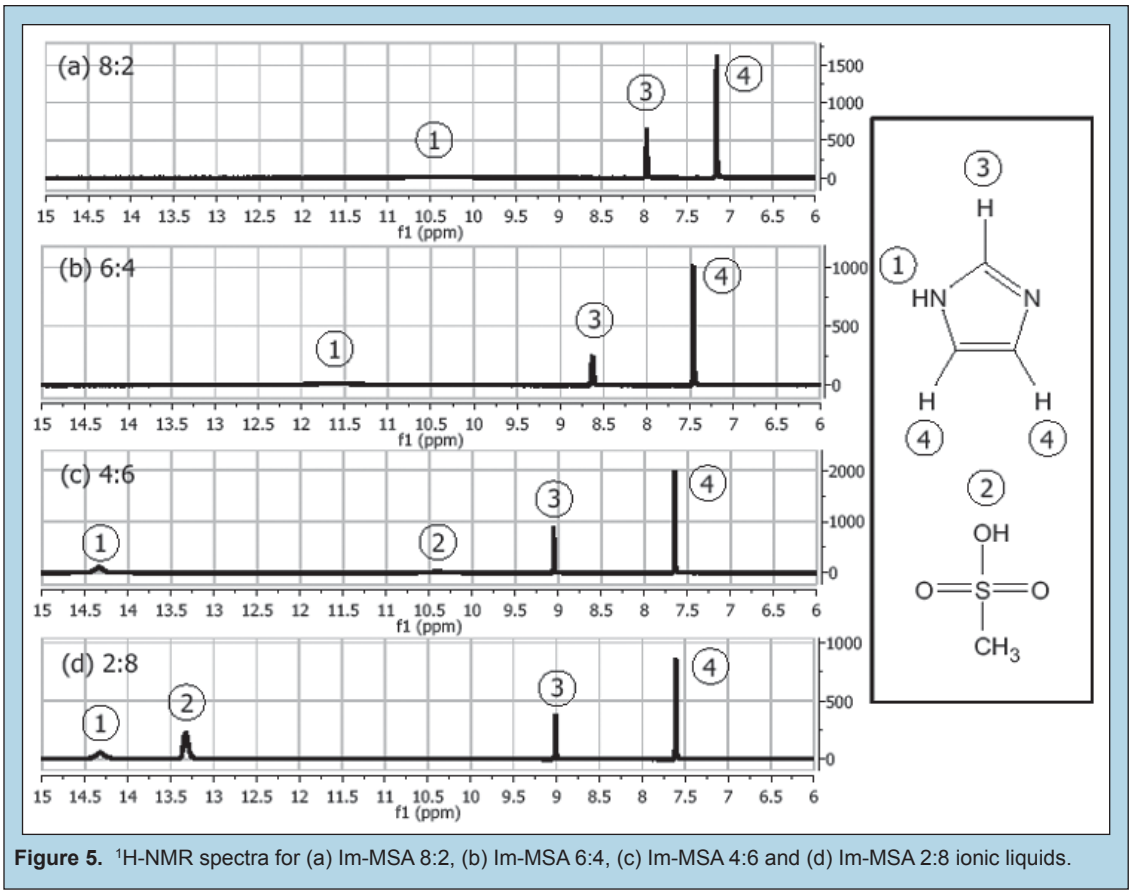

Figure 5. [1]H-NMR spectra for (a) Im-MSA 8:2, (b) Im-MSA 6:4, (c) Im-MSA 4:6 and (d) Im-MSA 2:8 ionic liquids.

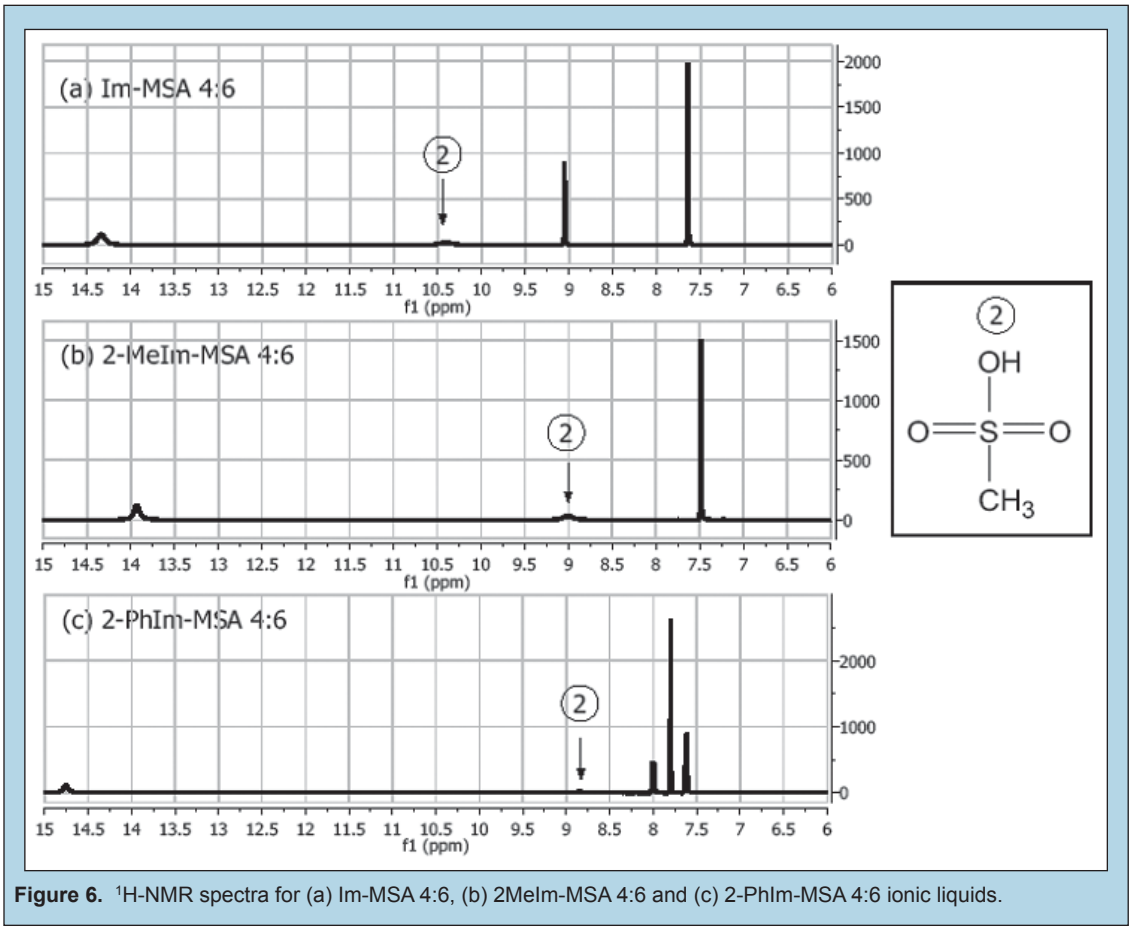

Figure 6. [1]H-NMR spectra for (a) Im-MSA 4:6, (b) 2MeIm-MSA 4:6 and (c) 2-PhIm-MSA 4:6 ionic liquids.

Im-MSA complex is farthest downfield. Figure 7 compares the chemical shift of the proton at position one of the Im-ring at all molar concentrations of three ionic liquid complexes. In Figure 7, the proton in the 2-PhIm-MSA complex is farthest downfield, while the proton in the 2-MeIm-MSA complex is farthest upfield.

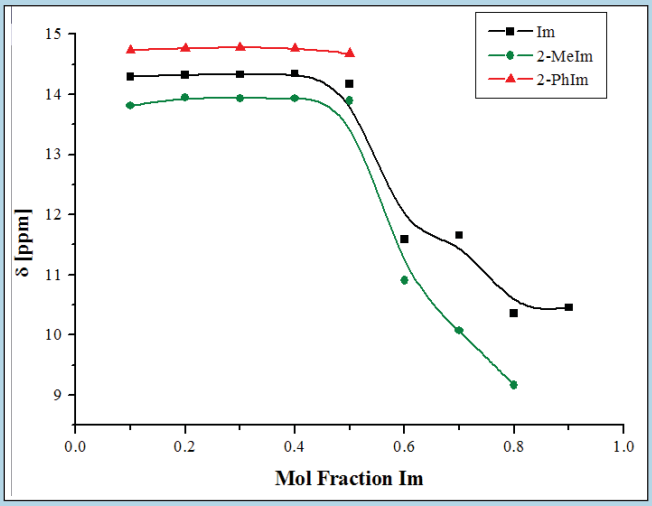

Figure 7. ^{1}H-NMR chemical shifts for all molar concentrations of Im, 2-MeIm and 2-PhIm at position one of Im-ring.

The dependence of ionic conductivity on temperature for all Im-MSA ionic liquid compositions is shown in Figure 8. The maximum conductivity reached was 4.35 x 10^{-2} S/cm, close to the benchmark goal desired by DOE. Conductivity decreased as temperature decreased, and base-rich compositions were the most conductive. The comparative conductivities of the 8:2 and 4:6 molar ratios of Im-MSA, 2-MeIm-MSA, and 2-PhIm-MSA as a function of temperature are shown in Figure 9. Unlike the Im-MSA complexes, acid-rich compositions of both the 2-MeIm-MSA and 2-PmIm-MSA complexes were more conductive than base-rich compositions. Figure 10 shows the three-dimensional structures of Im and 2-PhIm.

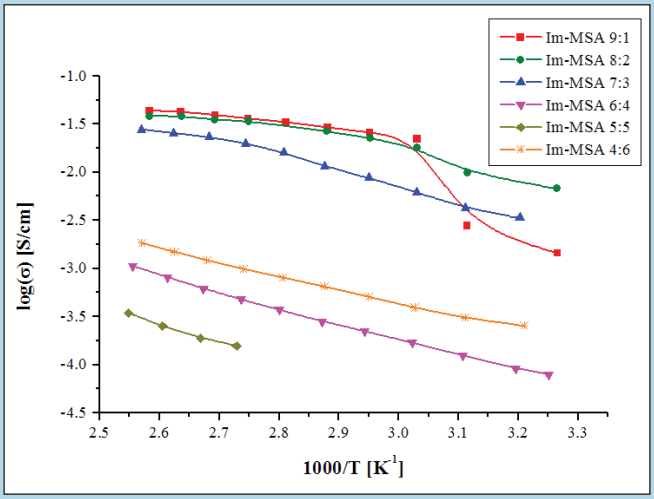

Figure 8. Ionic conductivity of Im-MSA ionic liquids as a function of temperature.

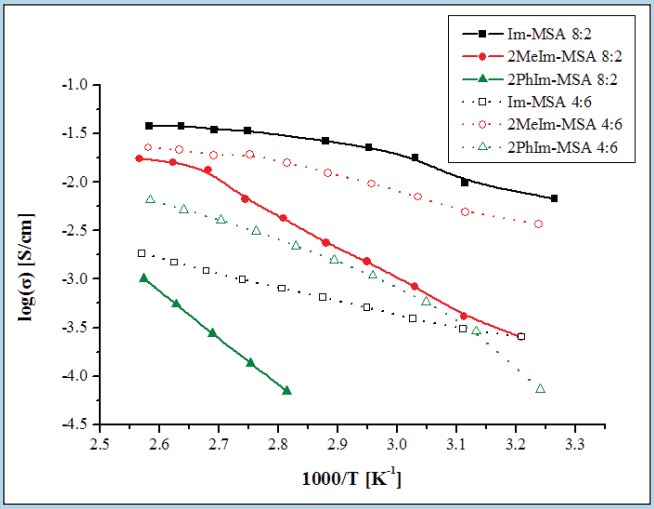

Figure 9. Ionic conductivities of Im-MSA, 2-MeIm-MSA and 2-PhIm-MSA ionic liquids at base-rich (8:2) and acid-rich (4:6) molar concentrations as a function of temperature.

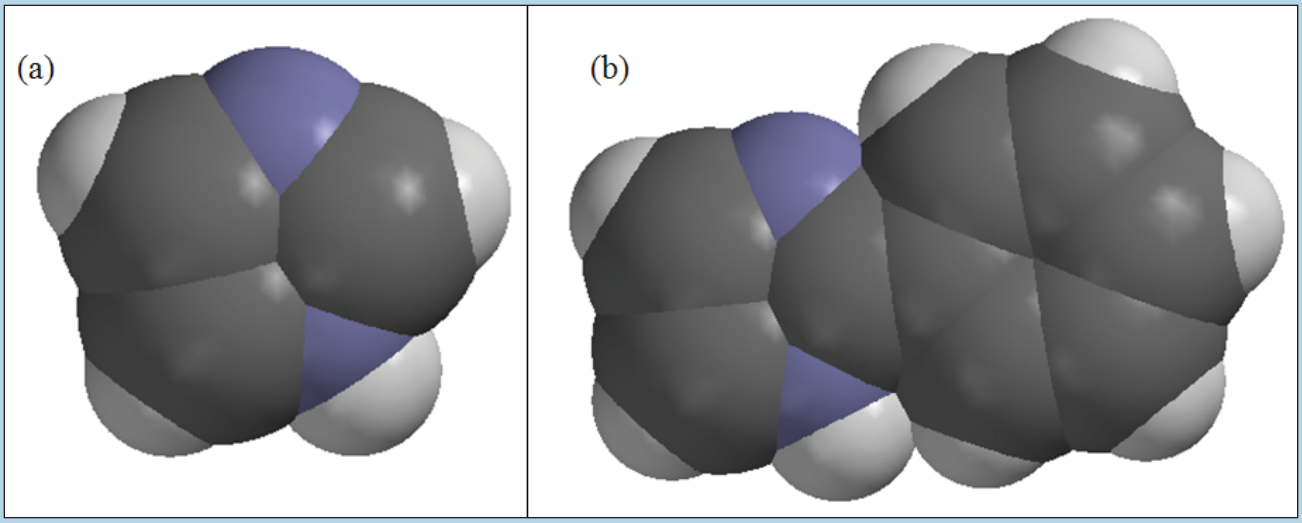

Figure 10. 3D structure of (a) Im and (b) 2-PhIm. Access to Im-ring is restricted by phenyl substituent.

Discussion and Conclusion

Thermal Behavior

The results from DSC testing showed that the melting point generally varied with molar concentration, and several patterns persist. The pure base maintained a higher melting point than when complexed with acid in unequal molar amounts. However, the equimolar salt had a significantly higher melting point than the other compositions. This result is due to the formation of a pure imidazolium salt with a very ordered crystalline structure, evidenced by the high heat of fusion (Table 2). Base-rich compositions were generally solids at room temperature, having higher melting points than acid-rich compositions, which were generally liquids at room temperature.

Results from the high-temperature stability testing using TGA show the expected weight losses. The equimolar composition showed a one-step weight loss above 300 °C, indicating high thermal stability. Im-rich compositions showed two step weight losses. The step at 150 °C represents the decomposition of excess Im, resulting in an equimolar salt which decomposes in the second step above 300 °C, similar to the 5:5 compositions. A greater molar ratio of Im present in the original salt results in a greater weight loss at the 150 °C step. The results demonstrate that temperature must be kept under 150 °C to maintain a base-rich ionic liquid, otherwise decomposition to an equimolar salt will occur. This data is accurate for ionic liquids only, in which the molecules are highly mobile; the incorporation of these molar ratios into a polymer membrane will change the thermal stabilities of the mixtures by tethering both the Im-ring and acid group to the polymer backbone.

^{1}H-NMR Chemical Shift

The proton transfer of the Grotthuss mechanism occurs at the number one position on the Im-ring. The chemical shift of this proton is important to understanding the electron density on the nitrogen atom. Figure 5 shows the ^{1}H signal moves further downfield as the molar concentration of acid increases, indicating that the proton is more localized on the Im-ring in an MSA-rich environment, evidence that the excess acid effectively protonates all the Im. Additionally, the chemical shift of the acidic proton on MSA appears only at MSA-rich compositions where excess MSA is present, shifting downfield and becoming more distinct. This further indicates that all the Im is protonated and the excess MSA does not dissociate.

Comparing the effects of the substituents in Figure 7, the data shows that the proton at position one of the Im-ring of 2-PhIm-MSA is shifted downfield compared to the proton on Im-MSA, while that of 2-MeIm-MSA is shifted upfield. The results confirm that the electron-withdrawing phenyl group attracts electron density away from the Im-ring, while the electron-donating methyl group contributes electron density. Therefore, the Im-ring of 2-PhIm is the most acidic, while the Im-ring of 2-MeIm is the least. The acidity is expected to directly affect the proton conductivity of the ionic liquids; the more acidic 2-PhIm forms weaker covalent bonds with protons, lowering the energy required to transfer that proton to the neighboring molecule.

Ionic Conductivity

A distinction must be made between ionic conductivity and proton conductivity. The methods used in this study measure ionic conductivity, a function of the mobility and concentration of all the charge carriers. The measurements include not only protons but all anions and cations. Therefore, the measured ionic conductivities include the MSA anion. Due to the nature of fuel cell operation, proton conductivity is of critical importance, so comparisons across different molar concentrations and across different bases must be made with consideration to the conductivity of the MSA anion. At acid-rich compositions, the MSA anion will contribute to ionic conductivity more so than at base-rich compositions. Comparisons across different bases must be made at identical molar ratios, to account for the concentration of MSA anions; however, the ionic conductivity cannot be negated. The impedance analysis method requires that an equal volume of ionic liquid be used for each measurement, which results in different molar amounts of acid and base being measured due to the differences in molecular size between Im (68.08 g mol^{-1}), 2-MeIm (82.11 g mol^{-1}), and 2-PhIm (144.2 g mol^{-1}). Therefore, the concentration of charge carriers varies between ionic liquids. With these considerations in mind, the following conclusions can still be drawn about the effect of the methyl and phenyl substituents on the proton conductivity of Im.

As seen in Figure 8, the conductivity of the Im-MSA ionic liquid increases with greater molar concentrations of Im. This result agrees with previous research, concluding that increased mole fractions of Im increase conductivity due to more rapid intermolecular proton transfer between the imidazole molecules [12]. They suggest that the method of proton transport is likely a combination of vehicle and Grotthuss-type mechanisms. The small temperature dependence of the Im-MSA 9:1, 8:2, and 7:3 ionic liquids is consistent with the operation of the Grotthuss mechanism over vehicular motion. Strong temperature dependence is more characteristic of the latter, as seen in the Im-MSA 6:4, 5:5, and 4:6 ionic liquids. Rotation of the Im molecule is less energetic than the movement of a proton carrier, and decreases in temperature have less of a negative effect on the conductivity of ionic liquids dominated by Grotthuss-type transport. Therefore, a shallow slope indicates the operation of the Grotthuss mechanism.

The comparative conductivities in Figure 9 show that the methyl and phenyl substituents affect the conductivity in different ways at base-rich and acid-rich compositions. At the base-rich 8:2 molar concentration, both groups retarded ionic conductivity of the Im-based ionic liquids. The ^{1}H-NMR shift of N-H in the Im-ring indicated decreased electron density on 2-PhIm-MSA in Figure 7, which is expected to facilitate proton-transfer between 2-PhIm molecules more easily; however, in such a base-rich environment, there is limited accessibility of the Im-ring to protons, a limiting factor in conduction. It must be noted that the phenyl group is significantly more bulky than either a proton or a methyl group; steric hindrance may have affected the accessibility of the nitrogen in the Im ring (Figure 10). As the model shows, access to the nitrogen is severely limited. Table 2 shows that the heat of fusion for 2-PhIm-MSA is lower than the heats of fusion for both Im-MSA and 2-MeIm-MSA, meaning that 2-PhIm doesn't pack as tightly. Therefore, while 2-PhIm may form weaker bonds with protons,

transfer is slowed by the less ordered structure of the ionic liquid, which does not support the Grotthuss mechanism well. Additionally, the phenyl group is less polarizable than the Im-ring, although it is of similar size. Therefore, the dielectric constant of the ionic liquid will be reduced, resulting in greater activation energy to dissociate the proton from MSA. This effect can be seen by a relatively steeper slope of 2-PhIm, which indicates a higher activation energy for conduction.

Interestingly, the conductivities of the acid-rich molar concentrations show a different trend. Both 2-MeIm and 2-PhIm showed increased conductivity over Im. The acid-rich environment produces an excess of protons, eliminating accessibility to protons as a limiting factor. Their great abundance compensates for the steric hindrance produced by bulky substituents, allowing for the electronic effects to predominate. As shown in Figure 7, the ^{1}H-NMR shift of 2-PhIm occurs farther downfield than Im at acid-rich compositions, confirming that the Im-ring is more acidic; the lowered electron density of 2-PhIm shows the expected result of increased ionic conductivity. The concentration of ions must also be considered. The large size of 2-PhIm reduces the concentration of ion carriers, a factor that reduces the ionic conductivity. Despite this, the 2-PhIm still showed increased conductivity over Im, further supporting the predominance of an electronic effect.

The increased conductivity of 2-MeIm-MSA over Im-MSA is a result that was not expected. A possible explanation is an increase in the number of MSA anions present in the ionic liquid, despite decreased proton conductivity. Figure 7 shows that the ^{1}H-NMR shift of 2-MeIm is shifted upfield compared to Im, meaning additional electron density increases the strength of the N-H bond, one that is more difficult to break. In the acid-rich environment, the excess of protons ensures that all 2-MeIm molecules are in an imidazolium form. Figure 6 shows that the chemical shift of the acidic proton on MSA is further upfield for 2-MeIm-MSA than for Im-MSA. This result signifies that the proton is more localized on the Im-ring of 2-MeIm, indicating a greater degree of dissociation. Consequently, the concentration of ion carriers is greater in the 2-MeIm-MSA ionic liquid than in the Im-MSA ionic liquid. The increase in ionic conductivity may not be due to increased proton mobility but instead increased ion carrier concentration. However, the 2-MeIm-MSA ionic liquid may facilitate proton transfer more easily because of a highly ordered structure, signified by its high heat of fusion shown in Table 2. Thus, Grotthuss-type proton transport is supported by a tightly packed ionic liquid, but hindered by the increase in electron density on N. Ionic conductivity, however, is increased over Im-MSA because of the higher concentration of ion carriers in the liquid.

Conclusion

The most significant discovery of this study is the differing effects of electron-withdrawing and electron-donating groups at base-rich and acid-rich compositions. It is important to note that several factors influence ionic conductivity, including electron density on the Im-ring, the degree of order in the ionic liquid, and the concentration of ion carriers. The ^{1}H-NMR chemical shifts demonstrate that 2-PhIm is more acidic than Im, which should enhance proton conductivity. However, steric factors become important at base-rich compositions where accessibility to protons is limited and a lowered dielectric constant increases the activation energy of dissociating the acid. At acid-rich compositions, with sufficient proton availability, the effect of the electron-withdrawing phenyl group predominated, thus increasing conductivity. The electron density on the Im-ring also affects the degree of dissociation of the imidazolium salt and the acid, changing the ion carrier concentration, thus changing the ionic conductivity.

The extension of the results of this study to polymer electrolyte membranes must be made cautiously. Tethering the base and acid groups to a polymer backbone would decrease the ionic conductivity due to the immobilization of ion carriers. The method of proton transport in a polymer structure is limited to a Grotthuss-type mechanism, which will be strictly influenced by the fluidity of protons in an Im-rich environment.

Future studies may help further elucidate electronic properties of such substituents by choosing less sterically-hindered bases, such as 2-chloroimidazole, which the synthesis for is described by [13]. Such a base would reduce the amount of steric hindrance produced by the substituent, as well as maintaining a high dielectric constant which would lower the activation energy of dissociating the acid. Studies using various bases, such as triflic acid, also may help find patterns between electronegativity and conductivity. Greater understanding of the electronic properties of Im-based ionic liquids will aid in the strategic development of a novel polymer with acceptable proton conductivity for use in automotive fuel cells. Such an advance is critical as modern society searches for a clean-burning replacement for fossil fuels.

Acknowledgements

This work could not have been achieved without the guidance and support of my mentor, Dr. John Kerr, who provided the opportunity to participate in this invaluable research experience. The helpful guidance of Yongzhu Fu and the other post-docs in the lab is also greatly appreciated. This opportunity was further supported by DOE and Lawrence Berkeley National Laboratory's Science Undergraduate Laboratory Internship program, and the Lawrence Berkeley National Laboratory's Center for Science and Engineering Education staff.

References

[1] D. Hissel, M.C. Péra and J.M. Kauffmann, "Diagnosis of automotive fuel cell power generators," *Journal of Power Sources*, vol. 128, pp. 239–246, 2004.

[2] "BC Transit contract for Air Liquide advances BC Hydrogen Highway," *Fuel Cells Bulletin*, vol. 2009, pp. 1–20, Jan. 2009.

[3] S. Ahmed and M. Krumpelt, "Hydrogen from hydrocarbon fuels for fuel cells," *International Journal of Hydrogen Energy*, vol. 26, pp. 291–301, 2001.

[4] "What are Batteries, Fuel Cells, and Supercapacitors?" *Chemical Reviews*, vol. 104, no. 10, pp. 4245–4269, 2004.

[5] I. Honma, H. Nakajima and S. Nomura, "High temperature proton conducting hybrid polymer electrolyte membranes," *Solid State Ionics*, vol. 154–155, pp. 707–712, 2002.

[6] P. Jannasch, “Recent developments in high-temperature proton conducting polymer electrolyte membranes,” *Current Opinion in Colloid and Interface Science*, vol. 8, pp. 106–92, 2003.

[7] O. Savadogo, “Emerging membranes for electrochemical systems Part II. High temperature composite membranes for polymer electrolyte fuel cell (PEFC) applications,” *Journal of Power Sources*, vol. 127, pp. 135–161, 2004.

[8] K. Kreuer, S. Paddison, E. Spohr and M. Schuster, “Transport in Proton Conductors for Fuel-Cell Applications: Simulations, Elementary Reactions, and Phenomenology,” *Chemical Reviews*, vol. 4, no. 10, pp. 4637–4678, 2004.

[9] N. Agmon, "The Grotthuss mechanism," *Chemical Physics Letter*, vol. 244, pp. 456–462, 1995.

[10] M. Susan, A. Noda, S. Mitsushimab and M. Watanabe, "Brønsted acid-base ionic liquids and their use as new materials for anhydrous proton conductors," *Chemical Communication*, pp. 938–939, 2003.

[11] A. Schechter and R. Savinel, "Imidazole and 1-methyl imidazole in phosphoric acid doped polybenzimidazole, electrolyte for fuel cells," *Solid State Ionics*, vol. 147, pp. 181–187, 2002.

[12] A. Noda, M. Susan, K. Kudo, S. Mitsushima, K. Hayamizu and M. Watanabe, “Brønsted Acid-Base Ionic Liquids as Proton-Conducting Nonaqueous Electrolytes,” *Journal of Physical Chemistry*, vol. 107, pp. 4024–4033, 2003.

[13] N. Jena, P. Kushwaha and P. Mishra, “Reaction of Hypochlorous Acid with Imidazole: Formation of 2-Chloro- and 2-Oxoimidzoles,” *Journal of Computational Chemistry*, vol. 29, pp. 98–107, 2008.

[14] B.S. Hickman, M. Mascal, J.J. Titman and I. Wood, “Protonic Conduction in Imidazole: A Solid-State ^{15}N NMR Study,” *Journal of the American Chemical Society*, vol. 121, pp. 11486–11490, 1999.